Research Article

Wear Resistance of (Diamond-Ni)-Ti6Al4V Gradient Materials Prepared by Combined Selective Laser Melting and Spark Plasma Sintering Techniques

Ramin Rahmani iD, Maksim Antonov, and Lauri Kollo

Tallinn University of Technology, Department of Mechanical and Industrial Engineering, Ehitajate tee 5, Tallinn 19086, Estonia

Correspondence should be addressed to Ramin Rahmani; ramin.rahmaniahranjani@ttu.ee

An approach of sintering 3D metal printed lattices and diamond nickel-coated particles is proposed which can be used for the production of tunnel boring machine (TBM) cutters and mining equipment blades. Nickel-coated diamond particles are mixed with titanium powder and incorporated into a lightweight Ti6Al4V (3D printed) lattice with the help of spark plasma sintering (SPS) method. Effect of Ti6Al4V lattices size, diamond particles size, and nickel coating layer thickness on wear resistance of composites is discussed. Functionally graded lattice (FGL) structures were produced by selective laser melting (SLM) method, representing an increasingly growing additive manufacturing engineering area introduced in material engineering. Impact-abrasive tribo-device (IATD), scanning electron microscopy (SEM), X-ray diffraction (XRD), energy-dispersive spectroscopy (EDS), and optical surface profiler (OSP) were used to characterize samples. An ab initio design of diamond-metal composite is based on the improvement of impact and abrasive wear resistance of Ti6Al4V by adding diamond particles and by applying of gradient lattice structure. The specimen with larger size of the diamond particle and thicker Ni coating has better wear resistance. In addition, ANSYS software simulations were done to analyze the effect of the presence of 3D printed lattice via nonlinear finite element AUTODYN solver under impact test. Diamond-based gradient composite material produced by combined SLM-SPS methods can be applied in applications where resistance against impact-abrasive wear is important.

1. Introduction

Ti6Al4V is the most applicable titanium alloy that has been extremely used in biomedicine, osteology, aerospace, marine, and additive manufacturing industries due to low density and high mechanical properties. Adding ≈6.75 wt. % of aluminum and ≈4.5 wt. % of vanadium to titanium makes it more applicable than pure titanium for corrosive wear resistance applications. Additive manufactured titanium alloys have motivated in deep *in vivo* corrosion research for recovering fractures of knee and hip bones [1]. It was recently demonstrated that 3D printed materials can provide improved tribological performance (lower coefficient of friction, stable performance) in sliding conditions [2]. Diamond is the hardest known, expensive, valuable, and versatile material for several industries. Synthetic polycrystalline diamond (PCD) is cost-effective and advantageous powder that can be coated by metals like cobalt, nickel, titanium, and copper and is usually used in grinding, polishing, and boring applications with sufficient cooling and without impacts. Diamond-containing metal matrix composites (MMCs) are made with the help of chemical/physical vapor deposition (CVD/PVD) techniques and they are considered because of their high thermal conductivity and mechanical properties [3]. Selective laser melting/sintering (SLM/SLS) is one of the new additive manufacturing techniques that is applied for production of complex metal shapes, lattice structures, and rapid prototyping. The SLM ability of creation lightweight metallic cellular structure with different unit cell structure, strut, and pore sizes is used as a more efficient approach to antishock/impact energy absorption, lightweight aerospace structure, electrothermal conductivity, fracture toughness enhancement, and acoustic insulation application [4, 5]. AISI 316L stainless steel, Ti6Al4V titanium, and AlSi10Mg aluminum are three highly demanded metal lattice structures due to high strength to weight ratio. Nowadays, Spark
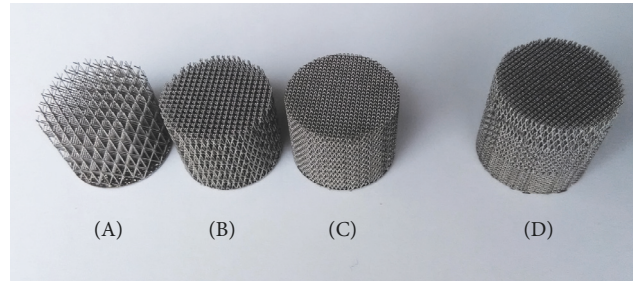
FIGURE 1: (A) Low, (B) average, (C) high volume fraction lattice structures, and (D) functionally graded lattice (FGL) structure used in the current research for samples No. 5 and No. 6 exclusively (diameter of lattice structures are 20 mm).

plasma sintering (SPS) is extensively used method based on pulsed DC electric current, high heating rates, programmable isostatic pressures, and short heating/cooling times [6]. The SPS process enables higher heating rate and sintering at lower temperature to provide consolidation of wide range of material including metals, ceramics, and cermets that is its main important advantage over conventional powder metallurgy techniques [7]. Phase degradation is almost avoided during SPS sintering. Pulsed electric current passes through a mold and conductive particles of material to be sintered. Based on pressure and temperature, it is possible to use graphite or tungsten mold and different diameter or thickness to realize desired production shape that is a suitable option in several industries. Temperature and pressure can be controlled by pyrometer/thermocouple and upper/lower punch electrode pushing force in a vacuum chamber, respectively. To avoid either graphitization of diamond or metal-coating surface oxidation, simultaneous increasing of temperature and pressure is required in SPS. Shrinkage of the powder, limited grain growth, and near-theoretical densification take place during sintering. Cellular lattice structure should be adjusted to take into account the shrinkage. The SLM parameters like cell size, lattice layer thickness, and laser current are important for the performance of the final material in test and field conditions. SLM method has been applied in recent study due to production possibility of metallic matrix in desired shapes (for example in SPS mold size or drag bits of tunneling machines) and possibility to fill spaces between the lattice rods with hard material particles (for example, diamond, cubic boron nitride, or WC-Co).

The main aims of this research were focused to optimize the composition of nickel-coated diamond and titanium powders for materials with and without titanium functionally graded lattice (FGL) structure to provide sufficient resistance against impacts and to improve abrasive wear resistance. FGL is a progressive multilayer lattice structure with different volume fraction section in longitudinal or circumferential directions so that the sections stand on each other or are embedded, respectively. Another novelty of current research is the combination of SLM and SPS methods to produce a new generation of multicomponent structures that can be used similarly to hard metals in various applications where wear resistance is of high importance. In this study, the influence of diamond particle and lattice cell sizes along with SPS parameters (temperature, pressure, and time) on tribological results is discussed. Samples were evaluated by combined impact-abrasive tribo-device (IATD), volumetric wear was measured with the help of optical surface profiler (OSP) analyzer, and composition of obtained materials was analyzed by X-ray diffraction (XRD) method.

2. Experimental Materials and Test Methods

Cellular lattice structures were fabricated from argon atomized Ti6Al4V Gd5 powders with size ≤ 45 μm and density 4429 kg/m^3 supplied by *TLS Technik GmbH.*, Germany. Polycrystalline diamond powder with 30 and 56 wt. % of nickel coating and fractions of 6-12, 20-30, and 40-50 μm were supplied by *Van Moppes & Sons Ltd.*, Swiss. Nickel coating usually contains 8-12 % of phosphorous and has 1455°C melting point (according to powder producer [8]). *Realizer* SLM50 3D metal printer machine (construction volume has a diameter of 70 mm and height of 80 mm, the thickness of layer was 20-50 μm, and argon consumption was 30 l/h) was used for preparing low, average, and high volume fraction (VF) Ti6Al4V lattices and FGL structures shown in Figure 1. Circumferential to longitudinal (C:L) cell size proportion for cylindrical lattices (Figures 1(A)–1(C)) with a diameter of 20 mm and initial height of 18 mm (final height of ≈10-12 mm) were 1:2 due to significant vertical shrinkage during SPS process. It was decided that final C:L and VF for lattice shown in Figures 1(A), 1(B), and 1(C) were 2:4 and 6 %, 1:2 and 15 %, and 0.75:1.5 and 24%, respectively. FGL structure (Figure 1(D)) is composed of three equal parts as a novel applicable lattice with 20 mm diameter and 18 mm initial height of sections with 1:1, 1:2, and 1:3 C:L proportion. The schematic of the desired FGL structure obtained by combined SLM and SPS is given in Figure 2. From bottom to top, reduction of Ti6Al4V lattice structure and enhancement of diamond particles before SPSing has been shown (Figure 2). Three most important parameters for printing of Ti6Al4V lattices by SLM method were set as follows: (1) laser current (LC=3000 mA, 72 W power), (2) exposure time (ET=600 μs), and (3) point distance (PD=1 μm). In addition, these parameters for solid parts (for example, 0.1 mm thick spacer between support and lattice) were as follows: LC=2500 mA, ET=25 μs, and PD=25 μm. The thickness of every layer was 25 μm and argon was applied as a protective gas during a process inside the printing chamber.
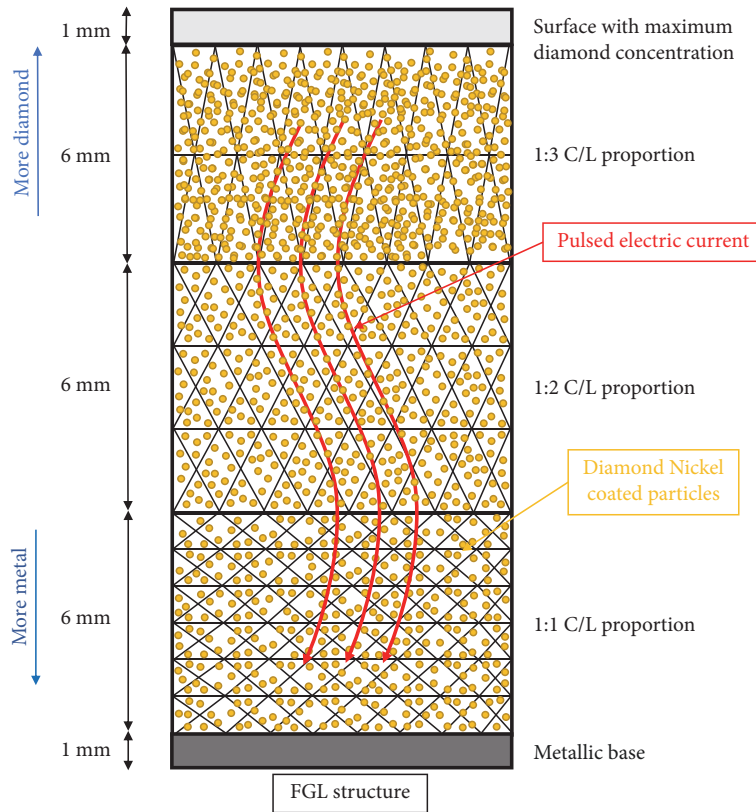
FIGURE 2: Schematic of material with FGL structure (during preparation before SPSing).

TABLE 1: Composition of samples and SPS sintering conditions.

Sample	Composition, wt. %	Diamond grain size, μm	Extent of Ni coating on D particle, wt. % [8]	Sintering pressure, MPa	Duration of sintering, min
1	29D-37Ni-34TA	40-50	56	50	9
2	29D-37Ni-34TA	6-12	56	100	6
3	29D-13Ni-58TA	40-50	30	50	9
4	29D-13Ni-58TA	20-30	30	100	6
5	26D-32Ni-24TA-18L	6-12	56	100	6
6	26D-11Ni-45TA-18L	20-30	30	100	6
7	100TA	Not-included	Not-included	50	10

- Preheating was performed at 260°C, 10 MPa and 6 Min. Sintering was done at 860°C for samples No. 1-6 and 1000°C for No. 7.
- D=diamond, TA= Ti6Al4V titanium alloy powder, and L is added in case of Ti6Al4V lattice.
- For No. 5 and No. 6, the average composition is stated due to gradient configuration.

In order to assess the influence of diamond particles size, nickel coating percentage (coating thickness), and lattice parameters, six samples were produced and are described in Table 1. The samples were designed so that each pair of samples can be compared to trace some specific effect. Sample No. 2 had finer diamond particles size than No. 1; heating/sintering time was shorter and the pressure was higher for sample No. 2 to reduce the risk of graphite formation. A similar effect can be studied with the help of samples No. 3 and No. 4 while these two samples were having thinner Ni coating on diamond particles that allows

tracing this effect as well. Samples No. 1-4 and No. 7 were lattice-free, whereas lattice-included No. 5 and No. 6 had similar composition (diamond grain size and nickel coating thickness) and sintering conditions as No. 2 and No. 4, respectively (Table 1). In order to provide similar diamond particle content in composite materials of No. 5 and No. 6 with Ti6Al4V lattice structure, the titanium powder content was reduced during SPS (Table 1).

The sintering device that was used for consolidation of nickel-coated diamond particles with titanium lattice structures was made by FCT Systeme GmbH. Such a device
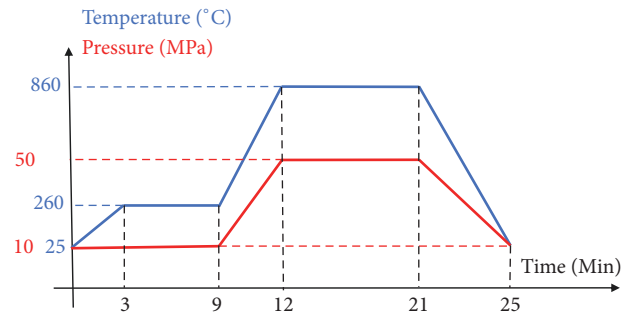
FIGURE 3: SPS conditions.

can enable 1000°C/min heating rate and 100 MPa (32 kN force for 20 mm diameter mold) pressure for samples. The machine is installed into glovebox form *MBRAUN Systeme GmbH* to perform all powder charging and weighting operations in a nitrogen atmosphere (to avoid their oxidation). Exemplary SPS sequence for sample No. 1 is presented in Figure 3. The main challenge regarding diamond particles incorporation into composites with a metallic or ceramic matrix with high melting temperature is discussed in the literature as graphitization phenomena [9]. In order to prevent graphitization, the SPS temperature of diamond-containing samples was kept below 900°C. However, some graphitization is not a major problem [10]. In order to remove the possible presence of water or hydrogen, the powders were preheated to 260°C and hold at 10 MPa pressure as it is shown in Figure 3. It was experimentally proved that such a step is improving consolidation and resulting in a lower level of graphitization and better properties (porosity, strength, and hardness) of the final composite material. Most important differences of SPS rather than conventional powder metallurgy techniques were fast heating, fast cooling, and simultaneous application of pressure and temperature. The increase in temperature to 860°C and pressure up to 50 MPa (Figure 3) enabled achieving high densification level (> 98 %).

The combined impact-abrasive wear tribo-device [11] was applied to test samples, with impact energy of 5.6 J and frequency of impacts being 27.5 Hz provided by impact generator (industrial hammer drill from Makita). The sample was experiencing reciprocative movement and was pressed (by the dead-weight system) against the rotating wheel (made from WC-Co) with a force of 49 N; linear abrasion velocity was 1 m/s. Ottawa sand (same as used in ASTM G65 standard [12]) was serving as abrasive. The particle size was 0.2-0.3 mm and feeding rate was the same as used during ASTM G65 test. The abrasive was supplied from a hopper through the pipe and nozzle into the contact region between wheel and sample. The duration of the test was 5 minutes corresponding to 300 m of sliding distance. The surface of the samples was cleaned by low angle incidence alumina particles jet after SPSing for SEM imaging. The observational study and characterization of samples were performed with the help of a Hitachi TM-1000 Scanning electron microscopy (SEM), 3D optical surface profiler (OSP) Contour GT-K0+ from Bruker, and X-ray diffraction (XRD) analyzer Bruker AXS D5005 equipped with Cu-Kα radiation. In addition, elements distribution in wear-tested region was mapped by energy-dispersive spectroscopy

(EDS) Zeiss EVO MA15 with INCA Energy 350 X-ray micro-analyser.

3. Results and Discussions

SEM images of nickel-coated diamond particles are shown in Figure 4. Nickel as a ductile transition metal was used as a binder metal is produced and tested metal matrix composite. Use of nickel-coated diamond particles was preferable in comparison with pure polycrystalline diamond due to resulting higher homogeneity of distribution of diamond in composite after sintering (Figure 5). Theoretically, Ti6Al4V FGL solid continuous cellular structure during SPS process should facilitate uniform heating due to its better electrical conductivity than the set of powder particles. It was tested and it can be suggested to keep maximum temperature of SPS procedure less than 900°C to avoid melting and escape of nickel from the gaps of the mold [13]. However, the volume of added nickel powder must be adjusted according to the requirements of the specific application. In this research, the content of Ni was varying between 11 and 37 wt. % due to variation in the thickness of Ni coating around diamond particles. Higher Ni content provides better sintering and densification for diamond particles.

In the SEM images (Figure 5) the dark diamond particles are visible. In Figures 5(a)–5(c) the difference of particles size is well seen and the homogeneity of distribution is acceptable. Sample No. 4 shown in Figure 5(d) has a less homogeneous distribution of diamond particles but the appearance of the surface of the samples can be influenced by its preparation (polishing) procedure before imaging. In addition, SEM micrograph of lattice structure in sample No. 6 is shown in Figure 6 after SPS and after IATD test. EDS color mapping (Figure 6(c)) shows distribution of elements. A random spectrum in tested area was chosen to define elements distribution. EDS elemental mapping results showed C 59.91 %, Ti 28.28 %, Ni 7.32 %, Al 1.87 %, V 1.34 %, P 0.79 %, Sn 0.36 %, and Si 0.13 % (all results in weight percentage).

XRD diffraction pattern (Figure 7) of sample No. 1 shows that material has diamond remained after the SPS process. There is also the minor presence of graphite that was either formed due to graphitization of diamond or appeared due to sintering in a graphite mold. There is also the minor content of new phases formed during SPS as result of reacting of initial components, namely, TiC and Al_2O_3, that are favorable for increasing of wear resistance of the composite material.

(a) Diamond-30 wt%Ni 20-30 μm

(b) Diamond-56 wt%Ni 6-12 μm

(c) Diamond-30 wt%Ni 40-50 μm

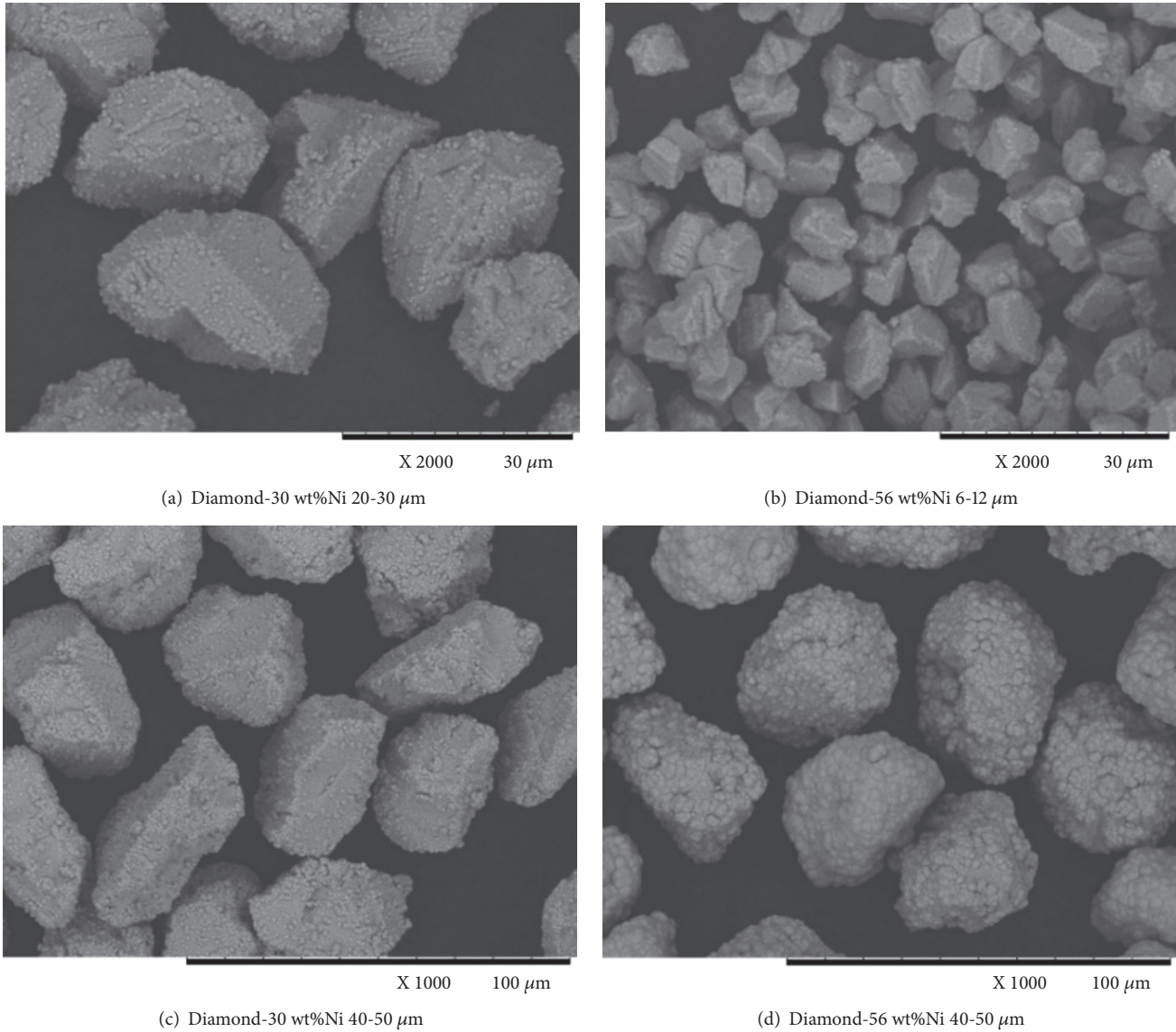(d) Diamond-56 wt%Ni 40-50 μm

Figure 4: SEM micrographs of nickel-coated diamond particles.

3D OSP was applied for surface scanning of samples and the profile of the area with a diameter of 17 mm around the tested area was obtained and analyzed by software to calculate the missing volume. In a photograph after IATD test, 3D OSP results of sample No. 1 (top and perspective views) are given in Figure 8. In order to illustrate the severity of the damage, it is possible to indicate that the maximum depth of the wear scar of sample No. 1 (29D-37Ni-34TA, 40-50 μm diamond grain size) was ≈300 μm. The red region shows intact zone while the blue zone was produced by sand particles passing between the wheel and sample during the IATD test. The results of wear rate measurements are shown in Figure 9. The IATD tests were repeated three times and results averaged. The best performer among the samples without lattice in impact-abrasive conditions was samples No. 1 and No. 2 (29D-37Ni-34TA, 6-12 μm diamond grain size) (if missing volume of material is considered). The sample No. 6 (26D-11Ni-45TA-18L, 20-30 μm diamond grain size) has illustrated better resistance than No. 5 (26D-32Ni-24TA-18L, 6-12 μm diamond grain size) among the samples with a lattice that is also shown in Figure 9. The best material (No. 1) had the largest size of diamond particles and the thickest Ni layer covering them. Material No. 3 (29D-13Ni-58TA, 40-50 μm diamond grain size) was also better due to larger diamond particle size (if compared to No.4 (29D-13Ni-58TA, 20-30 μm diamond grain size)). The same was valid for materials with lattice when No. 6 was better than No. 5. It could be concluded that, in case of materials with lattice, the size of diamond particles was more favorable than the thickness of Ni layer since No. 5 had thicker layer than No. 6.

In aggressive impact-abrasive conditions applied during the current test, the soft material No. 7 composed of pure titanium alloy had better resistance than No. 3 and No. 4. However, materials No. 5 and No. 6 with lattice were

(a) Sample No. 1

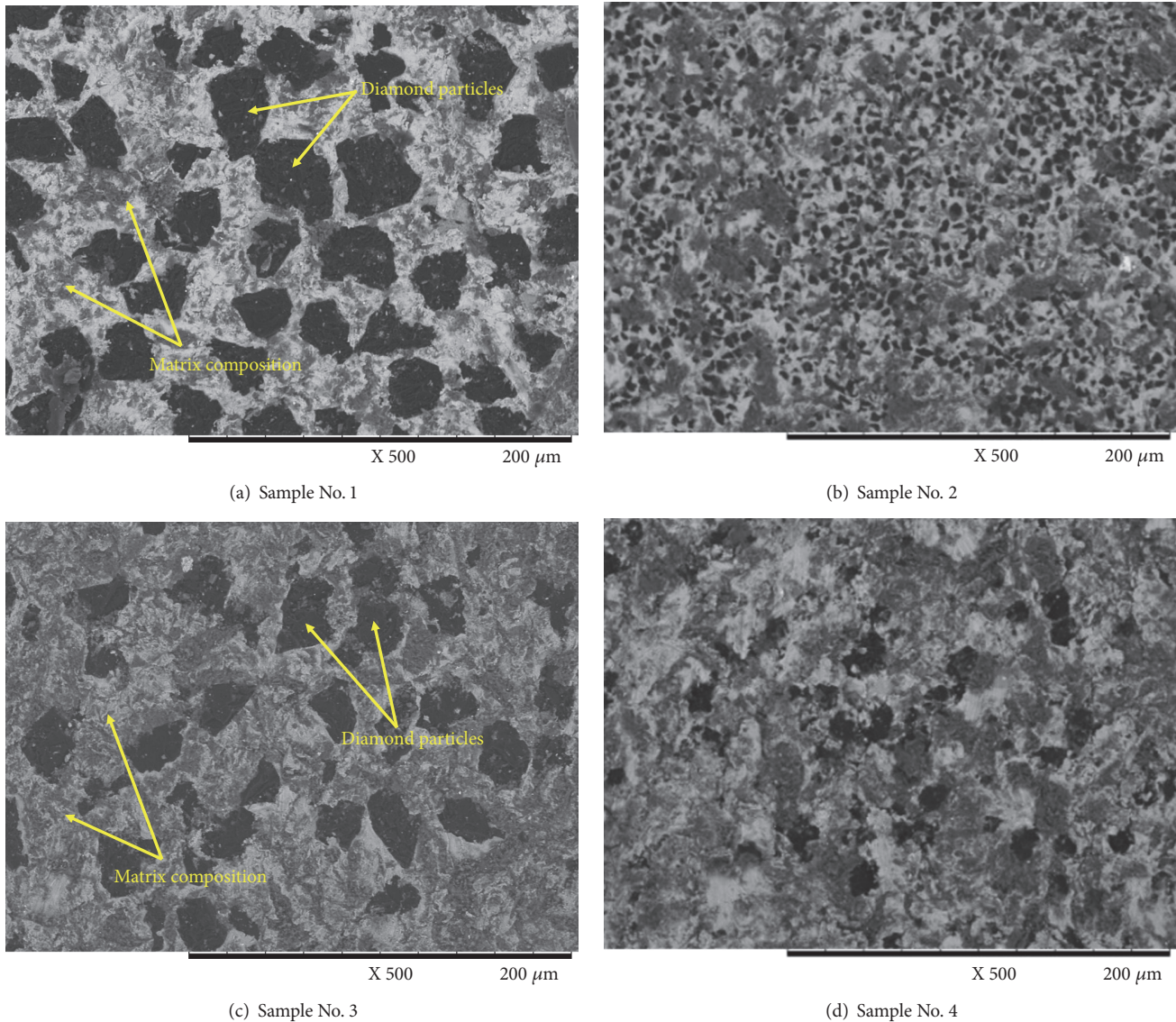(b) Sample No. 2

(c) Sample No. 3

(d) Sample No. 4

FIGURE 5: SEM micrograph of samples 1-4 after SPSing and cleaning by alumina particles jet.

having better wear resistance (than No. 7) in such impact-abrasive conditions and it is expected that in conditions with lower intensity or less frequent occurrences of impacts (typical for soft ground TBM applications) these materials will have significantly better wear resistance due to presence of diamond particles having extremely high resistance against abrasion.

The comparison between material No. 2 and No. 5 and between No. 4 and No. 6 provides the information about the effect of lattice on wear resistance. It is possible to conclude that in case of fine (6-12 μm) diamond particles (No. 2 versus No. 5) the addition of lattice is not favorable while in case of average (20-30 μm) size of diamond particles the use of lattice (No. 4 versus No. 6) provides significant improvement of wear resistance of the composite material. The composite material with a large size of diamond particles should be investigated in future since it should provide the best resistance in impact-abrasive conditions.

An important outcome of this study was to demonstrate the effect of diamond particle size, the thickness of the Ni coating, and the effect of metallic lattice structure on wear resistance. This was proved by XRD and by SEM images that diamond particles are present after the SPS process and after wear testing (Figures 5, 6, and 7). Various shapes of FGL structures can be produced by 3D printing and suitable SPS molds can be done in required shapes to develop required composite materials for industrial applications, i.e., wear resistant parts for mining or soft ground tunnel boring machines.

An advantage of FGL structure is that it is having more metal in bottom of sample for better connection of components (for example, insert to drag bit in TBM by bolting [14]), better absorption of impact due to increased ductility and gradual change of composition from prevailing very brittle diamond to prevailing ductile metal. High diamond

(a) Sample No. 6 (after SPSing and polishing)

(b) Sample No. 6 (after SPSing, polishing and testing)

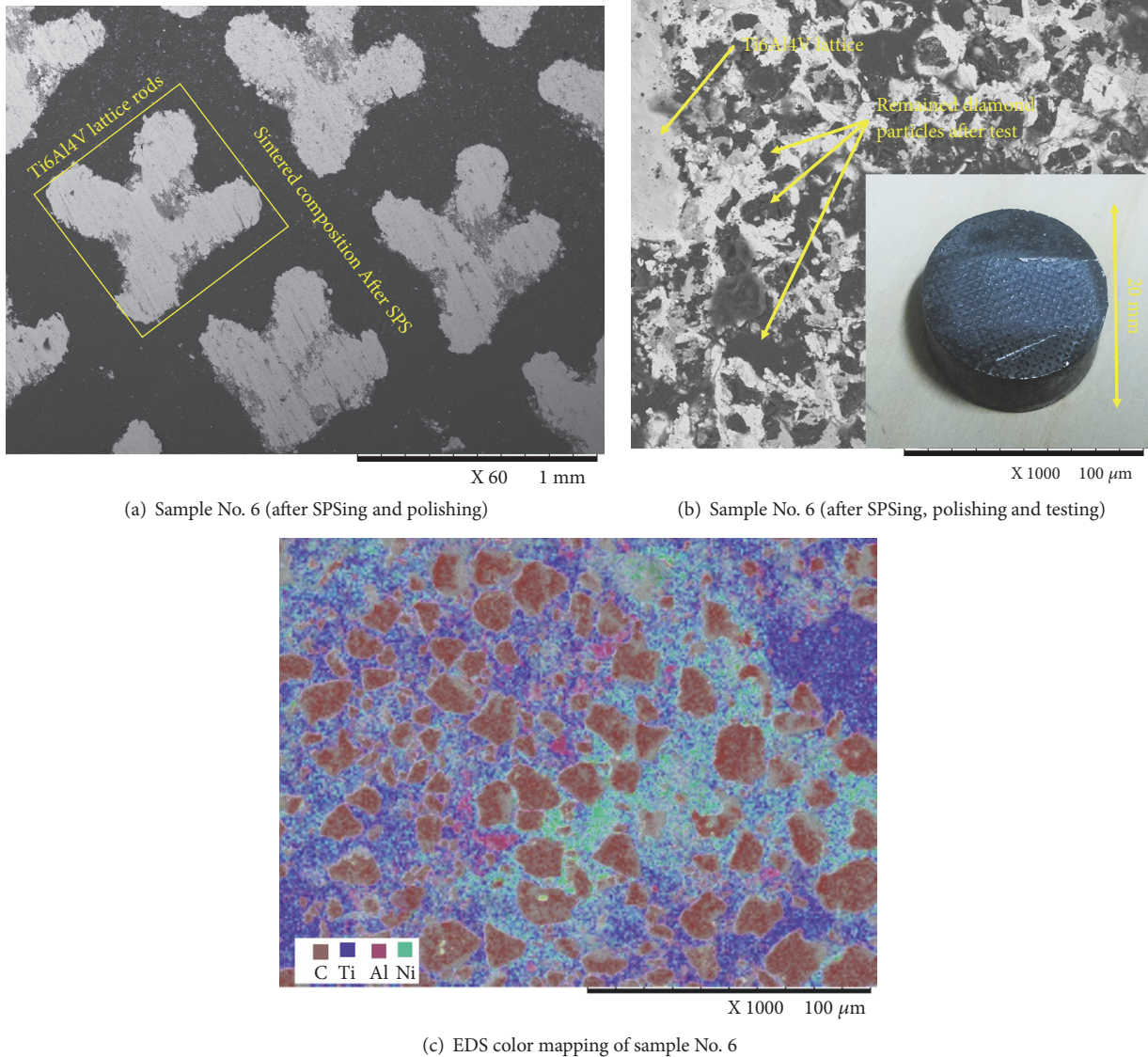(c) EDS color mapping of sample No. 6

FIGURE 6: SEM micrograph of sample No. 6 (a) after SPS and (b) after impact-abrasive test (c) EDS color mapping.

content in top layer provides extreme hardness and higher wear resistant.

Consequently, combinability of SLM and SPS techniques has enabled the creation of composites focused on the diversity of lattice structures, foreseeing all kind of possible future improvements in design and cost, by adjusting the fraction of desired phases to provide further improvement in hardness, fracture toughness, and corrosive behavior.

4. Simulation Study

In order to analyze the performance of the lattice structure, an impact test has been simulated using SOLIDWORKS design, ANSYS software, and AUTODYN solver. The first sample was simulated as made from solid diamond while the second one was simulated as being made from a metallic lattice with diamond located between the elements of the lattice. The wheel of the device was simulated as being made

from WC-Co cemented carbide and the lattice structure was modeled as a Ti6Al4V nonlinear finite element, respectively (Figure 10). Samples diameter was set as 20 mm and thickness as 10 mm. The simulation performed for material without lattice is shown in Figure 11. The second simulated sample having a 2×2×2 mm lattice scaffold is illustrated in Figure 12. During normal operation of the tribo-device (Figure 10(c)) [11] both rotation of the wheel (abrasive action) and impact between the sample and the wheel are provided but for current simulation, it was important to demonstrate the extreme case with impacting only (Figure 10(a)). The position of impacting was also changed. During the normal operation, the contact spot is located in the center of the sample while during the simulation the center of the impact spot was located exactly at the bottom edge of the sample to provide the most unfavorable leading resulting in brittle chipping or fracturing. The wheel was impacting the sample with the energy of 1000 and 5000 Joules (corresponding to different

A: TiC   D: Diamond
B: Ti6Al4V   E: Al_2O_3
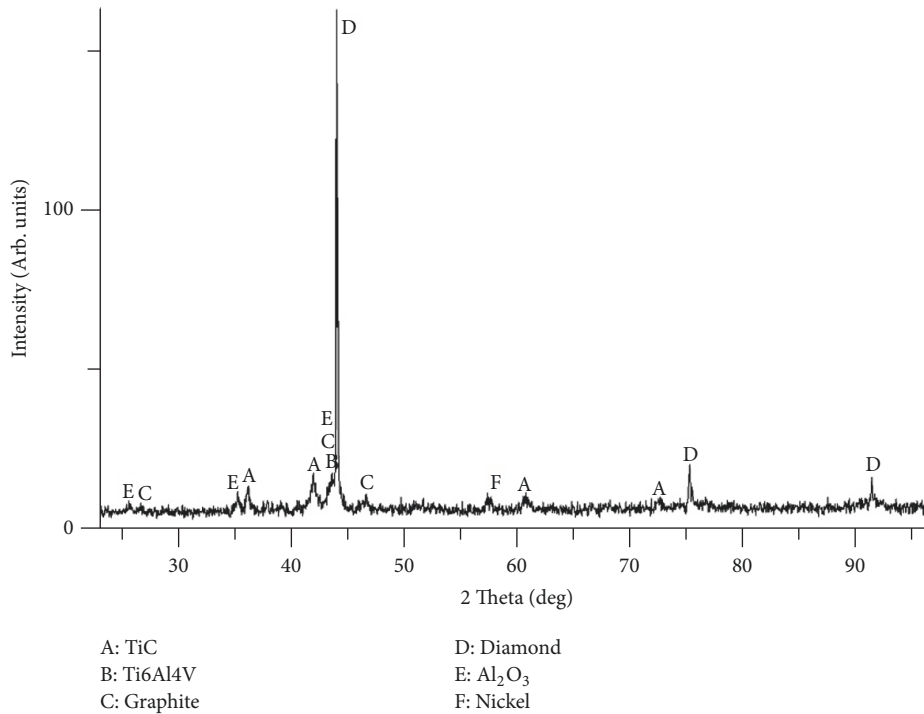C: Graphite   F: Nickel

FIGURE 7: An exemplary XRD diffraction pattern of sample No. 1 before wear testing.

velocities of the wheel); the analysis time and other boundary conditions were equal for both tests (with or without lattice). The von Mises equivalent stress comparison between samples without and with lattice structure is shown in Figures 11 and 12 for low and high impact energy. According to the results of both simulations (Figures 11 and 12), it is possible to say that in case of low impact energy the maximum Von Mises stresses are approximately ten times higher in case of pure diamond material than in case of a composite material with metallic lattice and diamond reinforcing particles. In case of high-energy impact, the pure diamond sample experienced fracturing and resulting extreme displacement of contact surface up to ≈3700 μm, while the composite material had only plastic deformation. Nonlinear finite element high-velocity contact modeling of sample's edge is a proper approach to evaluate energy absorption of materials [15]. The ability of impact energy absorption has grown up significantly with the addition of lattice structure as shown in Figure 13.

5. Conclusions

The present study is an attempt to introduce a new approach toward the production of wear resistant materials by the combination of selective laser melting and spark plasma sintering. The current work seeks to address the following results.

(1) The combined approach for the production of composite materials by the 3D printing of lattice (SLM) and sintering/consolidating (SPS) to incorporate metal-coated diamond particles has been described. It was concluded that it could be used for the production of soft ground TBM or mining parts.

(2) According to the results of wear testing in impact-abrasive conditions, either the larger size of the diamond particle or thicker Ni coating of diamond is favorable due to the reduction of the possibility of graphitization. The size of the diamond particles was found to have the strongest effect due to the harder removal of large diamond particles during the impact-abrasive process.

(3) Work on the creation of functionally graded lattice (FGL) composites is still in progress. It was found that diamond particles with larger size and thicker coating are more favorable for such materials. FGL structure provides the gradient change of metallic lattice extent from 0 % to 100 % that improves the resistance of such materials against impacts, allows predefining location of metallic phase responsible for ductility, and can enable fixation of such materials by welding or by bolting that is impossible for ceramics or other ultrahard materials.

(4) Finite element analysis was applied to illustrate benefits of lattice structure. Lattice-included material showed better response (stress, deformation, impact energy absorption, and the possibility of plastic deformation) than plain hard material against impact.

Data Availability

The materials, techniques, machines, references, and simulation data used to support the findings of this study are included within the article.

Conflicts of Interest

The authors declare that there are no conflicts of interest regarding the publication of this paper. The founding
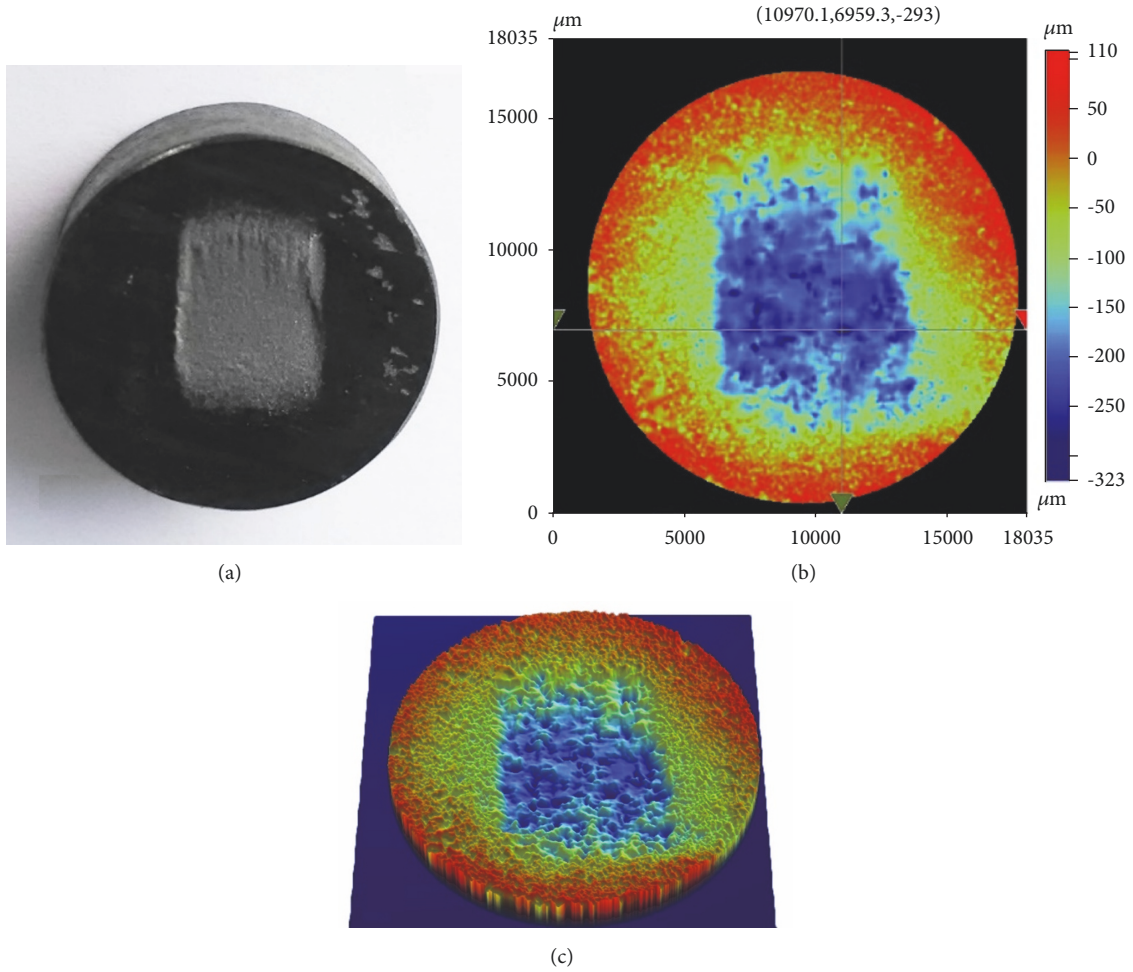
(a)

(b)

(c)

FIGURE 8: Sample No. 1 after impact-abrasive test (a) photograph, (b) 3D OSP contour micrograph, and (c) 3D OSP perspective micrograph.

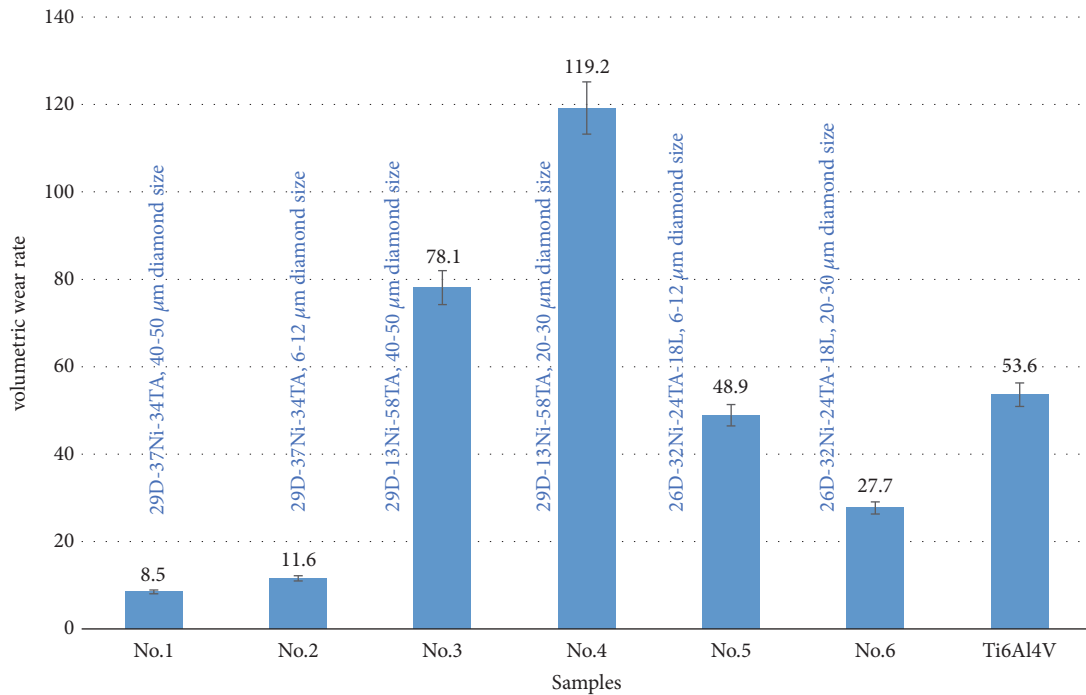FIGURE 9: Volumetric wear rate (missing volume) of samples during impact-abrasive test measured by 3D OSP, $\times 10^3$ μm^3.
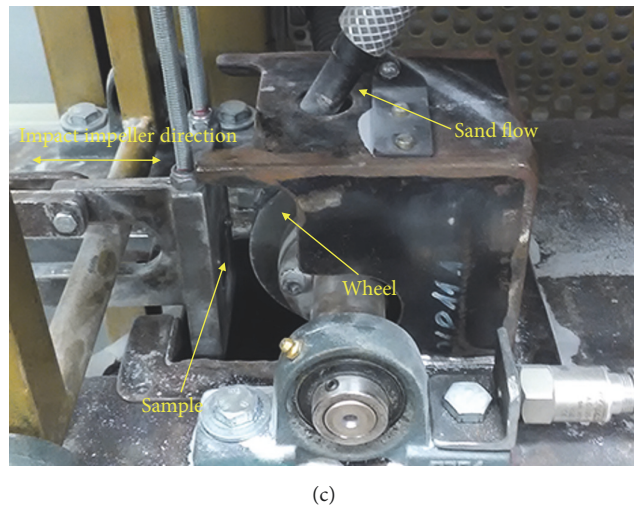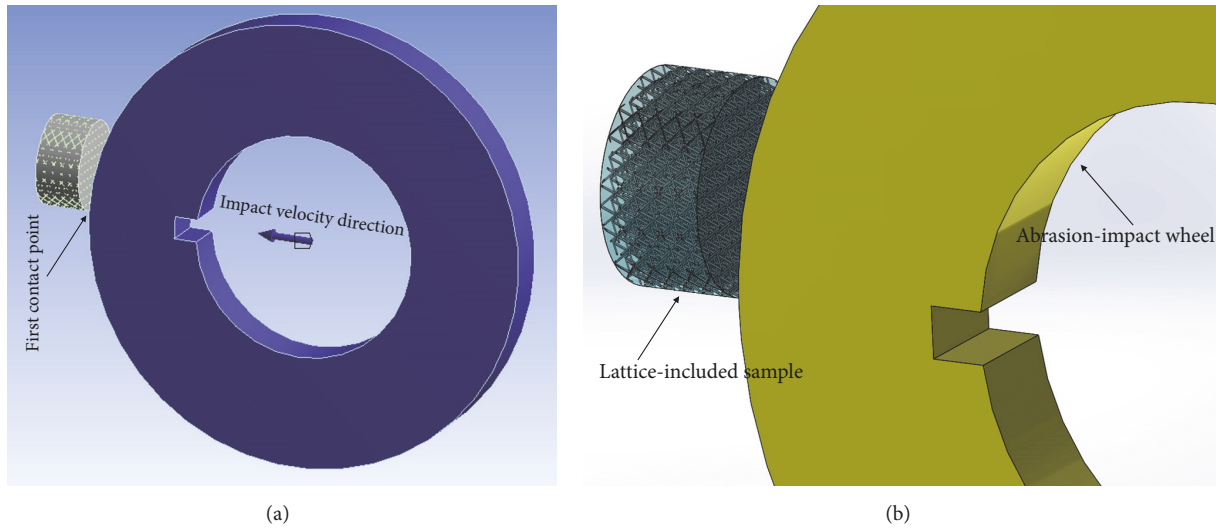
(a)

(b)

(c)

Figure 10: (a) Simulation mechanism, only horizontal impact motion, (b) schematic of wheel and lattice-included sample, and (c) position of sample and wheel in tribo-device laboratory [11].
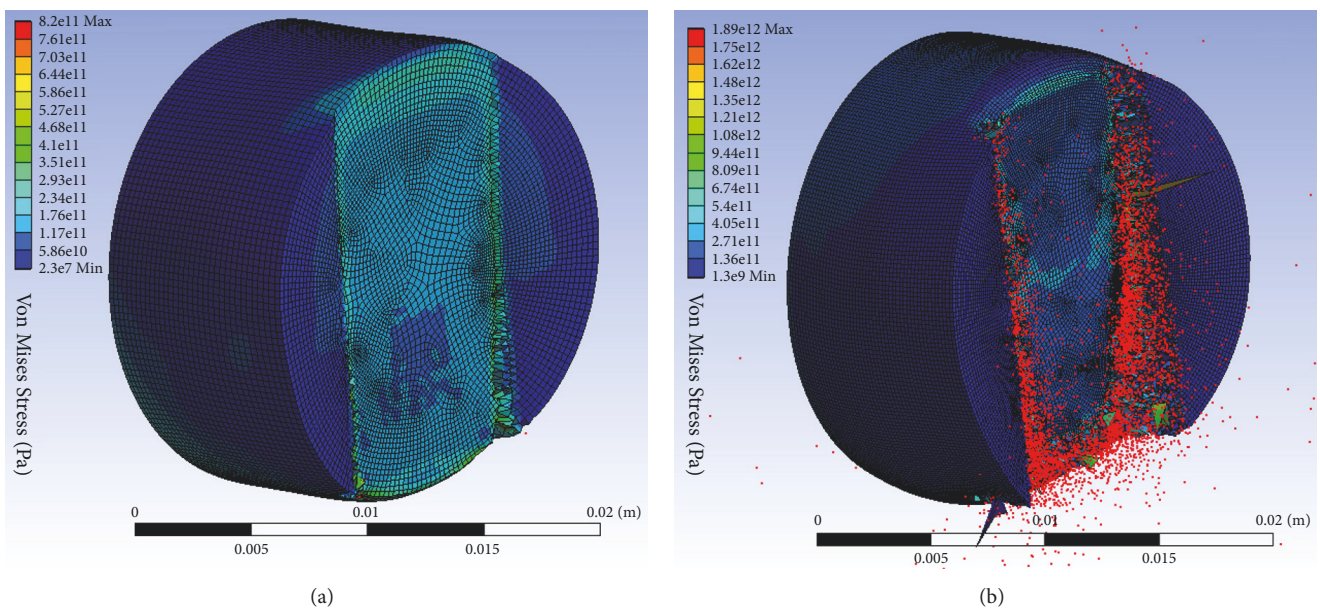

(a)

(b)

Figure 11: Stresses resulting from impact simulation of pure diamond sample without lattice: (a) 1000 J and (b) 5000 J impact energy.
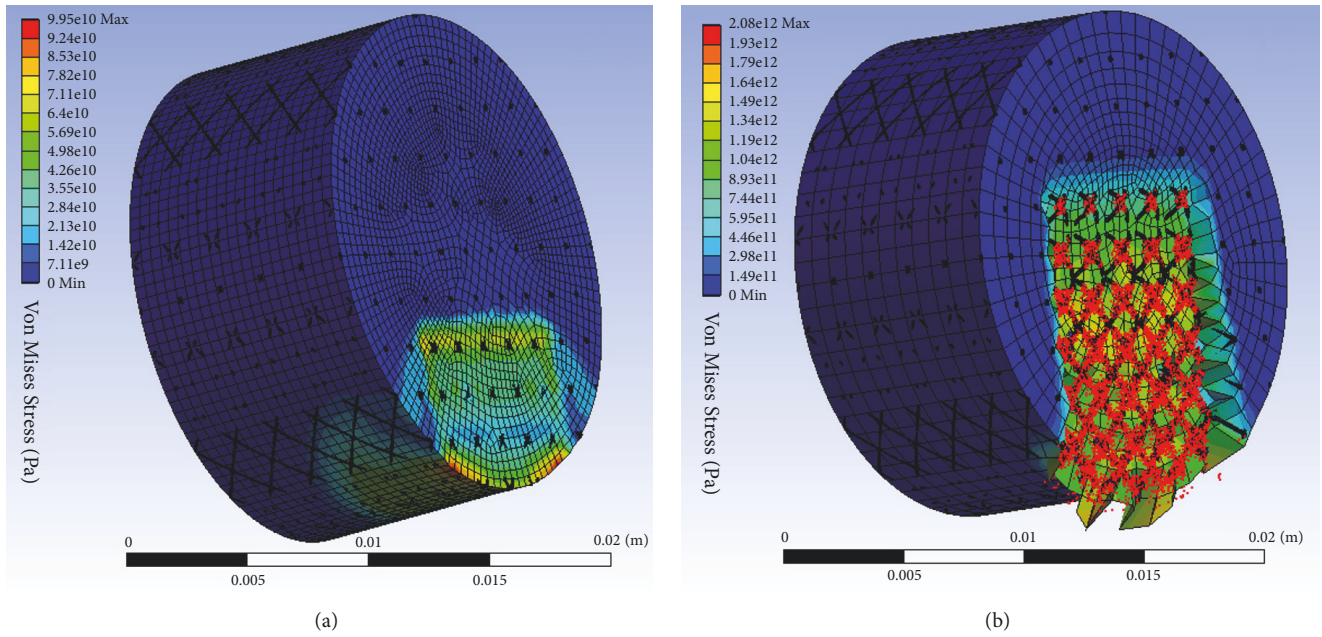
FIGURE 12: Stresses resulting from impact simulation of sample consisting of diamond and Ti6Al4V lattice structure: (a) 1000 J and (b) 5000 J impact energy.
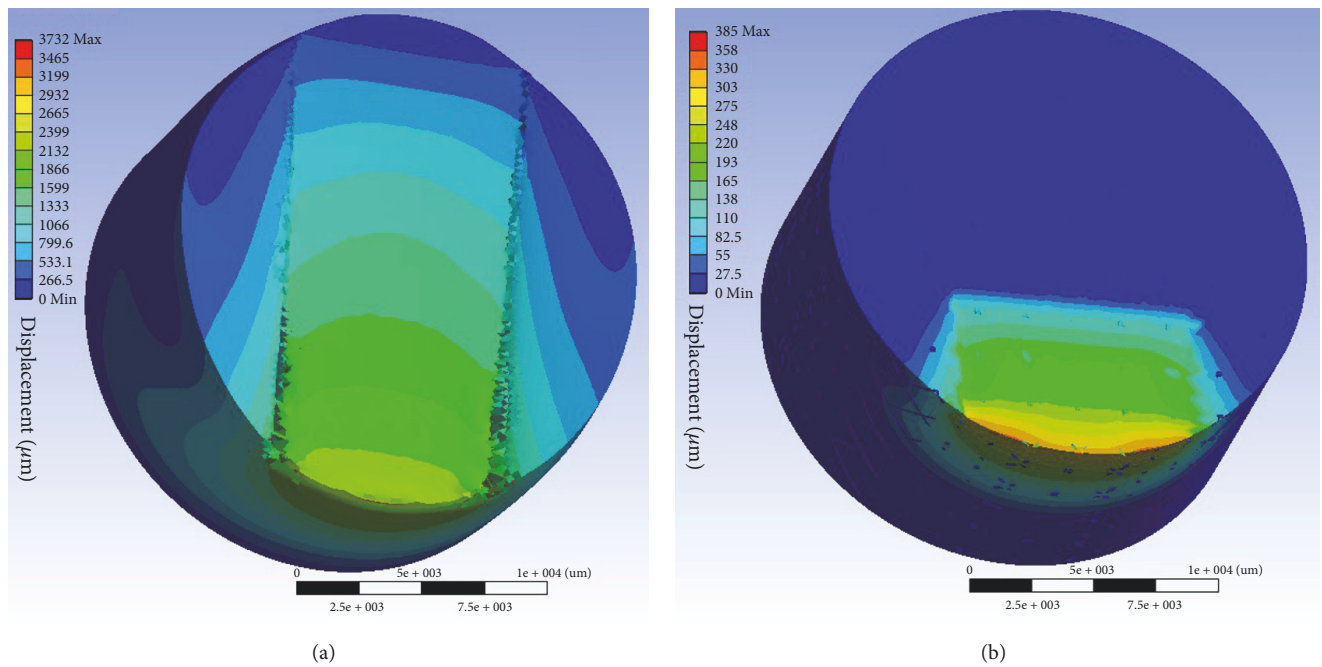

FIGURE 13: Displacement of 1000 J impact simulation of samples: (a) pure diamond and (b) diamond and Ti6Al4V lattice.

Authors' Contributions

Ramin Rahmani was responsible for methodology, experiments, software analysis, writing, investigation, and visualization,; Maksim Antonov was responsible for review, editing, project administration, and supervision,; Lauri Kollo was responsible for experiments, validation, and supervision.

Acknowledgments

References

[1] G. Li, L. Wang, W. Pan et al., "In vitro and in vivo study of additive manufactured porous Ti6Al4V scaffolds for repairing bone defects," *Scientific Reports*, vol. 6, article no 34072, 2016.

[2] Y. Holovenko, M. Antonov, L. Kollo, and I. Hussainova, "Friction studies of metal surfaces with various 3D printed patterns tested in dry sliding conditions," *Proceedings of the Institution of Mechanical Engineers, Part J: Journal of Engineering Tribology*, vol. 232, no. 1, pp. 43–53, 2018.

[3] D. F. Grech, S. Abela, M. Attard, and E. Sinagra, "Coating of diamond particles for production of metal matrix composites," *Surface Engineering*, vol. 29, no. 3, pp. 244–246, 2013.

[4] C. Yan, L. Hao, A. Hussein, P. Young, J. Huang, and W. Zhu, "Microstructure and mechanical properties of aluminum alloy cellular lattice structures manufactured by direct metal laser sintering," *Materials Science & Engineering A*, vol. 628, pp. 238–246, 2015.

[5] C. Yan, L. Hao, A. Hussein, P. Young, and D. Raymont, "Advanced lightweight 316L stainless steel cellular lattice structures fabricated via selective laser melting," *Materials and Corrosion*, vol. 55, pp. 533–541, 2014.

[6] Z. A. Munir, U. Anselmi-Tamburini, and M. Ohyanagi, "The effect of electric field and pressure on the synthesis and consolidation of materials: a review of the spark plasma sintering method," *Journal of Materials Science*, vol. 41, no. 3, pp. 763–777, 2006.

[7] A. Balbo and D. Sciti, "Spark plasma sintering and hot pressing of ZrB$_2$-MoSi$_2$ ultra-high-temperature ceramics," *Materials Science and Engineering A*, vol. 475, no. 1-2, pp. 108–112, 2008.

[8] http://www.vanmoppes.ch/en/.

[9] L. Jaworska, M. Szutkowska, P. Klimczyk et al., "Oxidation, graphitization and thermal resistance of PCD materials with the various bonding phases of up to 800°C," *International Journal of Refractory Metals and Hard Materials*, vol. 45, pp. 109–116, 2014.

[10] W. Z. Shao, V. V. Ivanov, L. Zhen, Y. S. Cui, and Y. Wang, "A study on graphitization of diamond in copper-diamond composite materials," *Materials Letters*, vol. 58, no. 1-2, pp. 146–149, 2004.

[11] M. Antonov, R. Veinthal, D.-L. Yung, D. Katušin, and I. Hussainova, "Mapping of impact-abrasive wear performance of WC-Co cemented carbides," *Wear*, vol. 332-333, pp. 971–978, 2015.

[12] "ASTM G65-04 standard test method for measuring abrasion using the dry sand/rubber wheel apparatus, annual book of ASTM standards," 2004, https://compass.astm.org/Standards/HISTORICAL/G65-04.htm.

[13] T. Borkar and R. Banerjee, "Influence of spark plasma sintering (SPS) processing parameters on microstructure and mechanical properties of nickel," *Materials Science and Engineering: A Structural Materials: Properties, Microstructure and Processing*, vol. 618, pp. 176–181, 2014.

[14] T. Camus and S. Moubarak, "Maintenance robotics in TBM tunnelling," in *Proceedings of the 32nd International Symposium on Automation and Robotics in Construction and Mining: Connected to the Future, ISARC 2015*, Finland, June 2015.

[15] P. Qiao, M. Yang, and F. Bobaru, "Impact mechanics and high-energy absorbing materials: Review," *Journal of Aerospace Engineering*, vol. 21, no. 4, pp. 235–248, 2008.